

Chemical Gardens

Formation and Evolution of Chemical Gradients and Potential Differences Across Self-Assembling Inorganic Membranes**

Fabian Glaab, Matthias Kellermeier, Werner Kunz,* Emilia Morallon, and Juan Manuel García-Ruiz*

Spontaneous physical compartmentalization of chemically distinct reaction chambers is a fundamental principle in living systems since the formation of the first protocells.^[1] However, self-organized partitioning of different chemical environments also occurs in purely abiotic systems and has been recognized in the course of iron and steel corrosion,^[2,3] Portland cement hydration,^[2,4] and the generation of ferro-tubes^[5] or hydrothermal vents.^[6] Another well-known example are chemical gardens, self-assembled structures forming when crystals of soluble multivalent metal salts are brought into contact with alkaline solutions of silicate or other specific anions.^[7,8] Instant deposition of a colloidal metal silicate skin on the crystal and ongoing dissolution of metal salt trigger a morphogenetic mechanism which is based on a combination of osmosis, buoyancy, and chemical reaction, and results in hollow tubular architectures.^[9]

The tube walls consist of metal silicates and hydroxides and separate, initially, an enclosed volume of concentrated acidic metal salt solution from a surrounding, strongly alkaline silica solution. These drastic variations in conditions between the two compartments render silica gardens interesting laboratory models for the study of spontaneously created gradients in membrane systems, as well as their application in materials science and biogeochemistry. Moreover, it has been claimed that they play a crucial role in proto-biochemistry.^[10,11] However, all previous discussions on the

importance of chemical gardens were largely based on morphological studies and ex situ characterizations of the formed tube material and the compartmentalization phenomenon.^[2,9,12–17] Consequently, detailed information on dynamic processes and, in particular, the time evolution of concentration gradients is still strongly limited.^[18] We have studied the development of silica gardens in situ by monitoring ion concentrations, pH, and the potential difference in the solutions on both sides of the membrane. Based on the collected data, we demonstrate the existence of long-lasting concentration and potential differences between the two reservoirs.

To enable concerted and reproducible analyses, a novel procedure for the preparation of standardized silica gardens was designed, and it relies on slow and controlled addition of dilute water glass to pressed tablets of metal halogenide salts. In this way, vertical hollow tubes were obtained (Figure 1a) with diameters of several millimeters and ends open to the

[*] Prof. Dr. J. M. García-Ruiz
Laboratorio de Estudios Cristalograficos, IACT (CSIC-UGR)
Avenida de Conocimiento s/n, 18100 Armilla, Granada (Spain)
E-mail: jmg Ruiz@ugr.es
Dr. F. Glaab, Prof. Dr. W. Kunz
Institut für Physikalische und Theoretische Chemie,
Universität Regensburg
Universitätsstr. 31, 93040 Regensburg (Germany)
E-mail: werner.kunz@chemie.uni-regensburg.de
Dr. M. Kellermeier
Physikalische Chemie, Universität Konstanz
Universitätsstr. 10, 78464 Konstanz (Germany)
Prof. Dr. E. Morallon
Instituto de Materiales, Universidad de Alicante
Ap. de Correos 99, 03080 Alicante (Spain)

[**] The authors thank R. Weikl, C. Fürst, J. Eiblmeier, and B. Bartel for experimental and analytical support. J.M.G.R. acknowledges financial support from the MICINN (projects MAT2006-11701 and CGL2010-16882) and the Factoria de Cristallización. E.M. thanks for financial support from MICINN and GV (projects MAT2010-15273 and ACOMP/2012/133).

Supporting information for this article is available on the WWW under <http://dx.doi.org/10.1002/anie.201107754>.

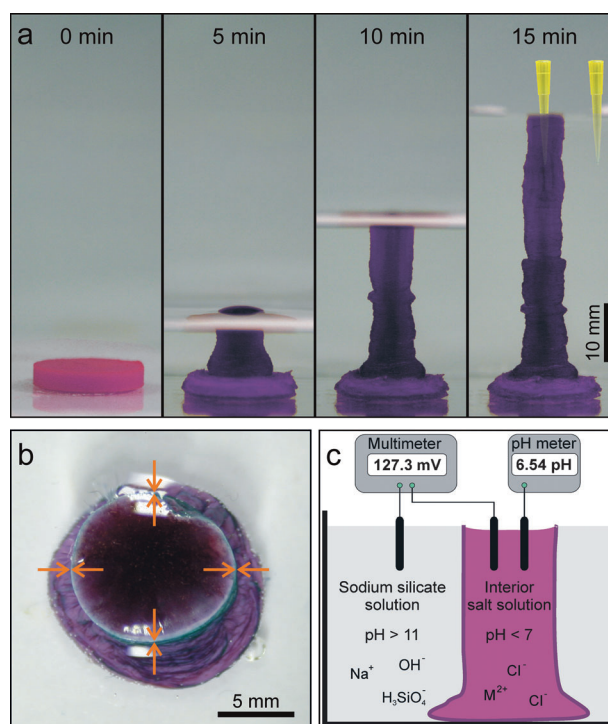


Figure 1. a) Formation of a tubular membrane with defined dimensions upon slow addition of silica solution to a tablet of CoCl_2 . Pipette tips indicate sampling of the inner and outer solution. b) Top view of the tube, showing its open end. Arrows mark the tube wall. c) Scheme of the experimental setup used for pH and ΔE_{H} measurements.

atmosphere (Figure 1b), thus granting facile access to the interior solutions.

Herein we discuss the results of experiments carried out with silica gardens based on Co^{2+} . However, similar trends were also observed with other metal ions such as Fe^{2+} or Fe^{3+} , thus suggesting that the traced processes are essentially independent of the metal salt. Concentration profiles of silicate, sodium, cobalt, and iodide ions obtained by sampling a silica garden prepared with CoI_2 are shown in Figure 2. Generally, enormous differences in the concentrations of all present species exist between the inner and outer solution

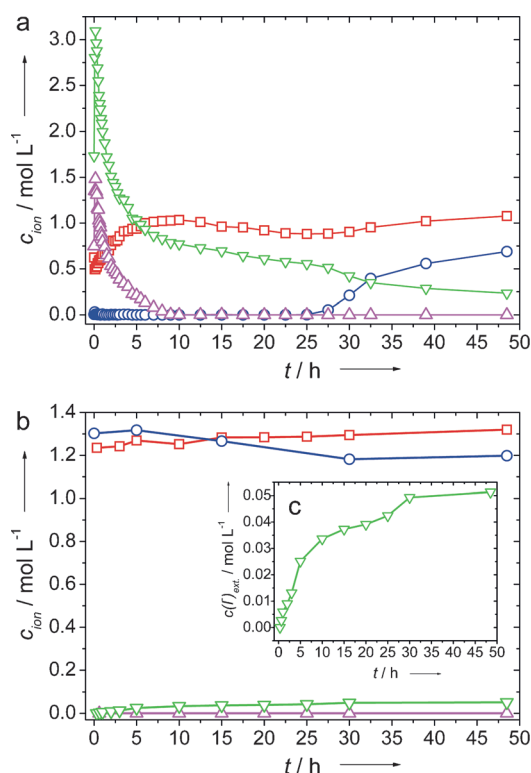


Figure 2. Progressions of the interior (a) and exterior (b) concentrations of cobalt (magenta), iodide (green), silicate (blue) and sodium (red) ions in silica gardens prepared with CoI_2 . c) Detailed evolution of the iodide concentration in the outer silica sol.

initially after tube formation, and they then fade with time owing to diffusion and precipitation processes.

In particular, no silicate is detected inside the tube for about 25 hours (Figure 2a). This finding can be explained by the drastic decrease of the pH value and, with it, the solubility of silica across the membrane at the beginning ($\text{pH}_{\text{ext}} \approx 11.5$, $\text{pH}_{\text{int}} \approx 6$, see Figure 3). Silicate ions trying to penetrate the tube wall therefore precipitate, forming amorphous, silica-rich material on the exterior surface of the tube as reported recently (see Section S1 in the Supporting Information for data on the structure and composition of the tube walls).^[14] In turn, once the inner solution is sufficiently alkaline, indiffusion of silicate species becomes possible and their concentration increases. The concentration of sodium in the interior volume is found to be as high as 0.5 M directly after completed tube preparation. This implies that a considerable

quantity of sodium ions (introduced with the outer silica solution) must have entered the inner solution before or while an intact membrane was formed. In a second step, Na^+ ions diffuse gradually through the wall, thus provoking an additional slow increase in the concentration during the first 10 hours (Figure 2a). Even after 48 hours, the concentrations of both silicate and sodium ions are still different in the two compartments, thus indicating that the system has not yet come to equilibrium.

The curve of the inner cobalt concentration exhibits a rapid initial increase (likely because of ongoing dissolution of the metal salt pellet), which, upon having reached a maximum after several minutes, turns into an exponential decrease down to values below the detection limit; the decrease is due to precipitation of metal hydroxides on the interior surface of the wall (see Section S1 in the Supporting Information). The concentration of iodide within the tube shows a similar temporal evolution as found for the cobalt ions, but values do not drop to zero. Instead, a slow decrease down to 0.25 M after 48 hours is observed. A comparison of the iodide concentration profiles in the two compartments reveals a reciprocal correlation over the entire period studied (Figure 2c). This is clear evidence that these anions are capable of diffusing through the tube wall. For all other elements (Na, Si, and Co), constant concentrations were found in the surrounding reservoir (Figure 2b) as a result of the large excess of water glass used, and the poor solubility of multivalent cations at high pH values.

Noticeable concentration gradients exist across the tube wall over periods ranging from 10 hours (Co) to more than 50 hours (I, Na, and Si). This observation suggests that the wall remained intact and neither in- nor outflow of relevant amounts through possible leaks occurred, so that the only feasible way of ion transport is diffusion. Thus, the walls of silica gardens cannot be regarded as true semipermeable membranes, as postulated in previous studies,^[2,9,15–17,19–21] but they rather allow bidirectional diffusion of multiple ionic species.

To confirm these results, the pH of both compartments was monitored over longer periods of time. While there were hardly any changes in the outer solution (because of the buffering ability of silica), the pH of the inner metal salt solution was found to evolve with time (Figure 3). Starting in

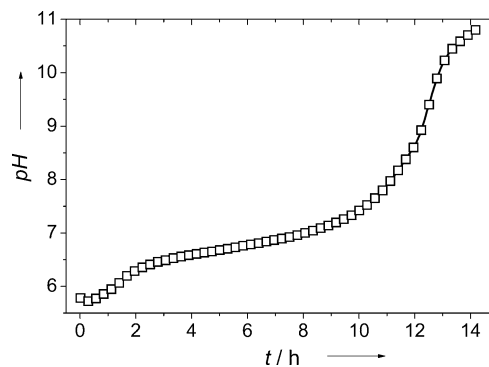


Figure 3. Time-dependent evolution of pH in the interior solution of a silica garden prepared with CoCl_2 .

the slightly acidic range ($\text{pH} \approx 6$), it first increases slowly to more or less neutral values within approximately 15 hours, before a much more distinct rise occurs until the pH eventually approaches alkaline values similar to those in the surrounding water glass reservoir ($\text{pH} \approx 11.5$). On the whole, the recorded pH progression strongly resembles the appearance of common acid/base titration curves, and therefore likely reflects the continuous removal of acidic Co^{2+} from the interior solution as a consequence of metal hydroxide precipitation—in line with the Co concentration data (Figure 2a). However, this requires diffusion of OH^- from the outer solution across the tube wall. Thus, our in situ pH measurements provide direct evidence for the permeability of silica garden membranes to hydroxide ions, as suggested in previous work.^[9,13,16,20]

The above findings strongly suggest that the electrochemical potential of the two solutions must be substantially different. Therefore, we have devised an experimental setup as depicted in Figure 1c to measure potential differences between the inner and outer compartment as well as their temporal evolution (Figure 4 and Section S3 in the Supporting Information for details). Indeed, remarkable potentials

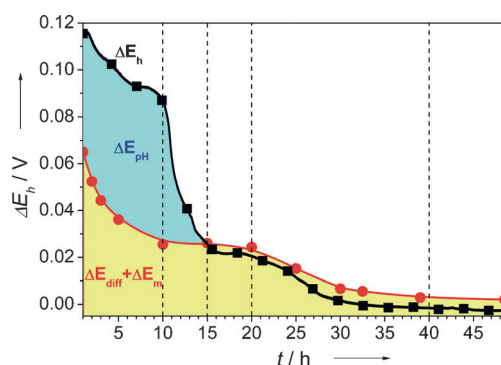


Figure 4. Electrochemical potentials in CoCl_2 -based silica gardens. The overall cell potential (ΔE_h) results from a combination of diffusion (ΔE_{diff}) and membrane (ΔE_m) potentials as well as a third pH-induced contribution (ΔE_{pH}).

($\Delta E_h \approx 115 \text{ mV}$) were measured immediately after tube preparation and found to decay with time in three distinct steps (black line; Figure 4). Each of them can be directly correlated to processes identified from the ion concentration and pH profiles: the first slight decrease of ΔE_h to approximately 90 mV (0–10 h) coincides with the period of Co^{2+} removal by hydroxide precipitation (Figure 2a), while the second rather distinct drop down to approximately 25 mV (10–15 h) corresponds to the steep increase of the interior pH value caused by the onset of OH^- in-diffusion (Figure 3). Eventually, the remaining potential difference is eliminated in a third step (20–30 h), which concurs with the beginning of silicate ion diffusion into the tube (Figure 2a), thus ultimately extinguishing any residual pH and concentration gradients, and hence also ΔE_h .

Contrary to the classical picture of the tube walls being semipermeable membranes, we propose a new model in which the properties of the walls are considered to be

a combination of the permeability characteristics commonly assigned to a diaphragm and a membrane. The rationale behind this approach is that, as a result of ongoing precipitation processes, the wall is either permanently (Co^{2+}) or temporarily (silicate, OH^-) impermeable to certain species (membrane characteristics), whereas it is continuously permeable for others (Na^+ , I^-/Cl^-) or allows ions to pass through freely once distinct gradients have diminished (silicate, OH^-) (diaphragm properties). On that basis, we have developed equations describing the measured potential differences as a combination of contributions originating from diffusion (ΔE_{diff}) and membrane (ΔE_m) potentials, as well as a third component (ΔE_{pH}) caused by the initially drastic pH gradient between the two reservoirs (see Section S2 in the Supporting Information for detailed explanations). With the aid of the concentration and pH data acquired in this work, the derived equations can be used to calculate the theoretically expected overall potential difference in the system as a function of time. Corresponding results show good agreement of the calculated curve progression with experimentally determined values (Figure 4 and Section S2). In particular, ΔE_h was found to be dominated by the pH-induced contribution, ΔE_{pH} , in the beginning (blue area; Figure 4) while, as soon as the inner pH value approaches levels close to those in the outer solution (after ca. 15 h), ΔE_{pH} tends to zero and the sum of membrane and diffusion potential alone accounts for the detected potential difference (yellow area; Figure 4).

Considering all gathered data, the evolution of chemical gradients in silica gardens can roughly be subdivided into four general stages, which are explained in the following for a system based on CoCl_2 (Figure 5). Stage 1 ($t < 10 \text{ h}$): Once compartmentalization and dissolution of the metal salt pellet are completed, no more fresh metal ions (M^{2+}) are released and metal hydroxide precipitation on the inner surface of the wall decreases their concentration. Concurrently, silica precipitates on the outer surface due to the acidic pH in the inside. Diffusion of chloride ions into the surrounding water glass reservoir is accompanied by counter-diffusion of sodium ions. All these parallel processes begin to reduce the concentration and pH gradients across the membrane. Stage 2 ($10 \text{ h} < t < 25 \text{ h}$): When all metal ions have been consumed by precipitation, the interior pH value is approximately neutral and thus still low enough to prevent transport of soluble silicate species through the membrane. Consequently, silica keeps on precipitating on the external surface. In turn, diffusion of hydroxide ions into the inner solution is now possible and subsequently increases its pH to alkaline values. Stage 3 ($25 \text{ h} < t < 50 \text{ h}$): Continued diffusion of OH^- strongly reduces pH differences between the two reservoirs, such that the solubility of silica inside the tube increases and unimpeded in-diffusion of silicate ions occurs. Stage 4 ($t > 50 \text{ h}$): After all diffusion processes have expired, the pH values and the concentrations of all present species are equal on both sides of the membrane and thermodynamic equilibrium is reached.

In summary, our experiments have shown that silica gardens are complex chemical systems operating out of equilibrium, forming after spontaneous separation of two solutions with drastic concentration differences. The chemical

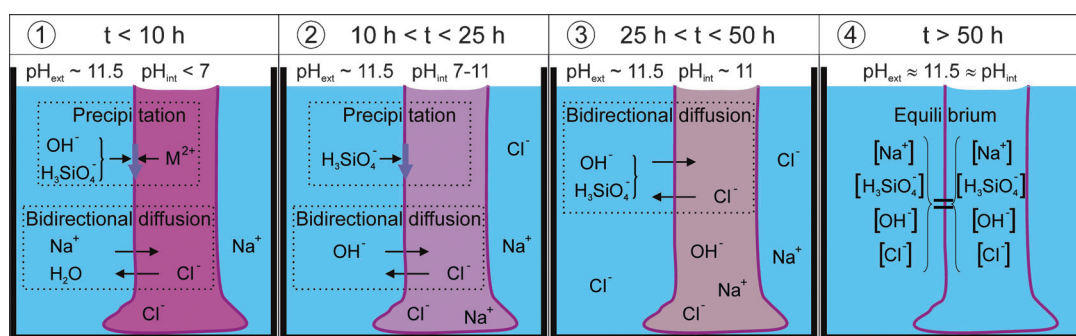


Figure 5. Scheme depicting the general stages proposed to describe the evolution of chemical gradients in silica gardens after completed tube formation and metal salt dissolution (see text for explanations). Note that, for the sake of simplicity, H_3SiO_4^- is meant to represent all soluble silicate species present in the system.

evolution of the system towards equilibrium was found not to extenuate once macroscopic formation of the well-known tubular structures is completed. Instead, a series of diffusion and coupled precipitation processes occur over time periods of up to days after preparation, thereby gradually relieving the initially generated gradients. The results of this study also demonstrate that the walls of silica gardens allow bidirectional and nonspecific ion transport, and thus fundamentally challenge the classical model of a semipermeable membrane. Moreover, our data readily explain previously reported variations in composition over the thickness of the wall, with silica-rich layers coating the outside and metal hydroxide crystals decorating the inside.^[14] Finally, we experimentally demonstrate the existence of appreciable (20–120 mV) and long lasting (more than one day) electrochemical potential differences between the two compartments, the origin of which is for the first time explained in detail in this work. We have shown that the overall period of precipitation and diffusion processes can be immediately correlated with the recorded potential curves, thus evidencing that differences in the (electro)chemical potential of the two compartments are the driving force for self-assembly ($\Delta_r G = -nF\Delta E$). To which extent these spontaneously created potential differences convert silica gardens into natural or artificial reactors able to catalyze either organic or inorganic reactions, and whether similar phenomena occur also in other self-compartmentalizing systems are matters still to be demonstrated and under investigation.

Experimental Section

Tube synthesis: Tablets ($m = 0.3\text{--}0.5\text{ g}$, $d = 13\text{ mm}$) of powdered and pressed metal salts ($\text{CoI}_2 \cdot \text{H}_2\text{O}$ and $\text{CoCl}_2 \cdot 6\text{H}_2\text{O}$, Merck, p.a.) were fixed at the bottom of a plastic beaker (120 mL). First, 10 mL sodium silicate solution (Sigma, diluted 1:4 (v/v) with Millipore water) were added at a rate of $\approx 1\text{ mL s}^{-1}$ with a plastic syringe, thus inducing the formation of a gel-like silicate membrane over the surface of the dissolving salt pellet. Addition of another 30 mL of the silica solution by a dosing apparatus (Unita I, Braun) at a constant rate of $1\text{--}10\text{ mL min}^{-1}$ (depending on the kind of metal salt) finally resulted in open vertical tubes (length: $\approx 20\text{ mm}$; diameter: $\approx 6\text{ mm}$).

Characterization: Samples taken after different times from the interior (10 μL) and exterior (100 μL) solutions were diluted with 10 mL water and analyzed by atomic emission spectroscopy on

a Spectroflame EOP instrument. Concentration calibrations were done by measuring elemental standard solutions (Fluka, Aldrich) diluted with water in ratios ranging from 1:20 to 1:1000 (v/v). The pH of the solutions was monitored using a glass microelectrode (InLab Micro, Mettler-Toledo). Time-dependent potential measurements were carried out by immersing platinum stick electrodes into both reservoirs. Data were recorded in steps of 5 s using a pH meter (Schott CG 843) and a multimeter (Metex M-3890D USB) connected to a PC.

Received: November 3, 2011

Revised: December 30, 2011

Published online: March 16, 2012

Keywords: compartmentalization · electrochemical potential · ion diffusion · membranes · self-assembly

- [1] P. A. Monnard, D. W. Deamer, *Anat. Rec.* **2002**, 268, 196–207.
- [2] R. D. Coatman, N. L. Thomas, D. D. Double, *J. Mater. Sci.* **1980**, 15, 2017–2026.
- [3] a) O. L. Riggs, J. D. Sudbury, M. Hutchison, *Corrosion* **1960**, 16, 260–264; b) J. D. Sudbury, O. L. Riggs, F. J. Radd, *Corrosion* **1962**, 18, 8–25.
- [4] a) D. D. Double, A. Hellawell, *Nature* **1976**, 261, 486–488; b) J. D. Birchall, A. J. Howard, J. E. Bailey, *Proc. R. Soc. London Ser. A* **1978**, 360, 445–453.
- [5] D. A. Stone, R. E. Goldstein, *Proc. Natl. Acad. Sci. USA* **2004**, 101, 11537–11541.
- [6] a) R. C. L. Larter, A. J. Boyce, M. J. Russell, *Miner. Deposita* **1981**, 16, 309–318; b) A. J. Boyce, M. L. Coleman, M. J. Russell, *Nature* **1983**, 306, 545–550.
- [7] C. W. J. Ross, *J. R. Soc. N. S. Wales* **1910**, 44, 583–592.
- [8] a) M. Copisarow, *Kolloid-Z.* **1929**, 47, 60–65; b) T. H. Hazlehurst, *J. Chem. Educ.* **1941**, 18, 286–289.
- [9] J. H. E. Cartwright, J. M. García-Ruiz, M. L. Novella, F. Otálora, *J. Colloid Interface Sci.* **2002**, 256, 351–359.
- [10] a) S. Leduc, *The mechanism of life*, Rebman & Co., New York, **1911**; b) A. L. Herrem, *Science* **1942**, 96, 2479; c) E. F. Keller, *Making Sense of Life: Explaining Biological Development with Models, Metaphors, and Machines*, Harvard University Press, Cambridge, **2002**.
- [11] a) M. J. Russell, R. M. Daniel, A. J. Hall, J. A. Sherrington, *J. Mol. Evol.* **1994**, 39, 231–243; b) W. Martin, M. J. Russell, *Philos. Trans. R. Soc. London Ser. B* **2003**, 358, 59–85.
- [12] T. S. Sørensen, *J. Colloid Interface Sci.* **1981**, 79, 192–208.

- [13] E. Bormashenko, Y. Bormashenko, O. Stanevsky, R. Pogreb, G. Whyman, T. Stein, Z. Barkay, *Colloids Surf. A* **2006**, 289, 245–249.
- [14] a) J. Pagano, S. Thouvenel-Romans, O. Steinbock, *Phys. Chem. Chem. Phys.* **2007**, 9, 110–116; b) J. H. E. Cartwright, B. Escibano, S. Khokhlov, C. I. Sainz-Díaz, *Phys. Chem. Chem. Phys.* **2011**, 13, 1030–1036; c) J. H. E. Cartwright, B. Escibano, C. I. Sainz-Díaz, *Langmuir* **2011**, 27, 3286–3293; d) J. H. E. Cartwright, B. Escibano, C. I. Sainz-Díaz, L. S. Stodieck, *Langmuir* **2011**, 27, 3294–3300.
- [15] a) D. Balköse, F. Özkan, U. Köktürk, S. Ulutan, S. Ülkü, G. Nisli, *J. Sol-Gel Sci. Technol.* **2002**, 23, 253–263; b) K. Parmar, H. T. Chaturvedi, M. W. Akhtar, S. Chakravarty, S. K. Das, A. Pramanik, M. Ghosh, A. K. Panda, N. Bandyopadhyay, S. Bhattacharjee, *Mater. Charact.* **2009**, 60, 863–868; c) C. Collins, W. Zhou, A. L. Mackay, J. Klinowski, *Chem. Phys. Lett.* **1998**, 286, 88–92.
- [16] C. Collins, W. Zhou, J. Klinowski, *Chem. Phys. Lett.* **1999**, 306, 145–148.
- [17] a) C. Collins, G. Mann, E. Hoppe, T. Duggal, T. L. Barr, J. Klinowski, *Phys. Chem. Chem. Phys.* **1999**, 1, 3685–3687; b) C. Collins, R. Mokaya, J. Klinowski, *Phys. Chem. Chem. Phys.* **1999**, 1, 4669–4672.
- [18] a) L. Roszol, O. Steinbock, *Phys. Chem. Chem. Phys.* **2011**, 13, 20100–20103; b) L. M. Barge, I. J. Doloboff, L. M. White, G. D. Stucky, M. J. Russell, I. Kanik, *Langmuir* **2012**, Article ASAP.
- [19] a) S. Thouvenel-Romans, O. Steinbock, *J. Am. Chem. Soc.* **2003**, 125, 4338–4341; b) S. Thouvenel-Romans, W. Van Saarloos, O. Steinbock, *Europhys. Lett.* **2004**, 67, 42–48; c) S. Thouvenel-Romans, J. J. Pagano, O. Steinbock, *Phys. Chem. Chem. Phys.* **2005**, 7, 2610–2615; d) J. J. Pagano, T. Bánsági, O. Steinbock, *J. Phys. Chem. C* **2007**, 111, 9324–9329; e) I. Uechi, A. Katsuki, L. Dunin-Barkovskiy, Y. Tanimoto, *J. Phys. Chem. B* **2004**, 108, 2527–2530; f) H. Yokoi, N. Kuroda, Y. Kakudate, *J. Appl. Phys.* **2005**, 97, 10R513.
- [20] D. E. H. Jones, U. Walter, *J. Colloid Interface Sci.* **1998**, 203, 286–293.
- [21] J. J. Pagano, T. Bansagi, O. Steinbock, *Angew. Chem.* **2008**, 120, 10048–10051; *Angew. Chem. Int. Ed.* **2008**, 47, 9900–9903.